

Supporting Information for

Computational Study of the Addition of Methanethiol to 40+ Michael Acceptors as Model for the Bioconjugation of Cysteines

Anna M. Costa,* Lluís Bosch, Elena Petit, and Jaume Vilarrasa*

Organic Chemistry Section, Facultat de Química, Universitat de Barcelona, Diagonal 645, 08028 Barcelona, Catalonia, Spain

Computational methods (additional details)	SI-2
Complementary results	SI-2
Full Schemes of the main text	SI-3
Relevant M06-2X/6-311+G(d,p) equilibrium geometries (Cartesian coordinates)	SI-7
Experimental	
NMR spectra of 1 -D	SI-10
Treatment of 1 with NaH	SI-11
Migration of AcCysOMe from 1 to 2	SI-12
Exchange of thiolates in the maleimide adducts (mechanisms)	SI-13
References	SI-14

Computational methods (additional details)

All the calculations were carried out with the Gaussian 16 package.⁵¹ Some were repeated with Spartan'18 or with ORCA.⁵² The M06-2X/6-311+G(d,p) method was used everywhere.⁵³ Many structures were first calculated at the MP2/6-31G(d)//B3LYP/6-31G(d) level, which in our hands⁵⁴ is the approach that afforded us the lowest performance/cost ratio for the appropriate ordering of sets of conformers and which we mention as MP2 or MP2/6-31G(d). Thus, comparisons were often established between MP2/6-31G(d) and M06-2X/6-311+G(d,p) total energies of the different molecules and anions; in other words, the several possible or reasonable conformers of every species were calculated and compared at these two levels. For large molecules, with many low-energy conformations, we confirmed that there were no significant differences (around 0.0001–0.0003 au, less than 0.2 kcal/mol) between M06-2X/6-311+G(d,p) and M06-2X/6-311+G(d,p)//M06-2X/6-31G(d), so that sometimes we took advantage of this approach for saving computing time.

The scaling factors used in Scheme 2 for the estimation of ΔH° and ΔG° from the frequency calculations are those published⁵⁵ for several M06-2X methods [but not for M06-2X/6-311+G(d,p), so a mean value of 0.95 was taken] and for B3LYP/6-31G [and then the correction was added to the MP2/6-31G(d)//B3LYP/6-31G(d) values].

The effect of polar solvents was estimated by optimization of the equilibrium geometries and total energies with the implicit-solvent models included in the programs. The CPCM and SMD methods implemented in Gaussian 16 were tested (see Extended Scheme 2). As indicated in the corresponding Schemes, the comparisons were frequently carried out by means of Spartan'18 (CPCM); in some cases, SS(V)PE, a symmetrized version of IEF-PCM, and SM8 were used as well. Orbital drawings were also obtained from Spartan'18.

The stationary points were characterized by evaluating the harmonic vibrational frequencies at the optimized geometries to verify that minima and transition states have zero and one imaginary frequency, respectively.

We also carried out a few single-point calculations at higher levels, mainly at CCSD(T)/6-311+G(d,p), in order to check whether the energy differences (among the conformers or between reactions) predicted at the DFT level were maintained. Generally, this was the case.

It deserves comment that M06-2X predicts that reactions in Scheme 2 of the main text are more exothermic than CCSD(T)/6-311+G(d,p) does; however, the gaps are relatively small

[–29 kcal/mol vs. –28 kcal/mol with the CCSD(T)/6-311+G(d,p) for the addition of MeSH to *N*-methylmaleimide]

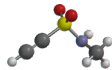
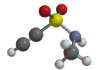
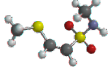
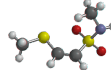
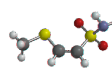
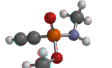
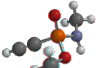
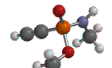
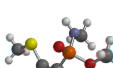
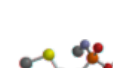
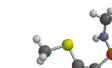
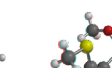
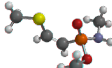
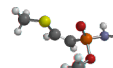
[–43 kcal/mol vs. –40.5 kcal/mol with the CCSD(T)/6-311+G(d,p) for the addition of MeSH to *N*-methylpropynamide],

so that for discussions and comparisons we always used the M06-2X results.

What matters are the relative reaction energies.

Complementary results

In Figure 1 of the main text, to locate each lowest-energy conformer, several species required a complete conformational analysis at an appropriate level of theory. A paradigmatic example is shown below ($\text{HC}\equiv\text{C}-\text{SO}_2\text{NHMe}$ and the *Z* isomer of $\text{MeS}-\text{CH}=\text{CH}-\text{SO}_2\text{NHMe}$). A more complex case follows, where the presence of tetrahedrally substituted P atom, viz. the non-planar chiral structures of phosphonamidates $\text{HC}\equiv\text{C}-\text{PO}(\text{OMe})\text{NHMe}$ and $\text{MeS}-\text{CH}=\text{CH}-\text{PO}(\text{OMe})\text{NHMe}$, increases the number of possible conformers. Only the most stable conformers are depicted in both cases. The relative energies, with regard to each lowest-energy conformer, are indicated in bold (in kcal/mol). As explained in the main text, the ΔE values were always obtained from the total energies of the corresponding lowest-energy conformers, for the sake of simplification.

							
M06-2X/6-31G(d)	–720.37638 1.1	–720.37820 0.0	–1159.08838 0.5	–1159.08914 0.0	–1159.08672 1.5		
M06-2X/6-311+G(d,p) ^a	–720.50646 1.6	–720.50901 0.0	–1159.26142 0.0	–1159.26121 0.1	–1159.25854 1.8		
M06-2X/6-311+G(d,p)	–720.50671 1.6	–720.50921 0.0	–1159.26156 0.0	–1159.26136 0.1	–1159.25869 1.8		
M06-2X/6-311+G(d,p)-w ^b	–720.52652 2.2	–720.53000 0.0	–1159.28746 0.0	–1159.28533 1.3	–1159.28295 2.8		
							
M06-2X/6-31G(d)	–703.56607 1.3	–703.56718 0.6	–703.56809 0.0	–1142.26656 0.0	–1142.26538 0.7	–1142.26482 1.1	–1142.26370 1.8
M06-2X/6-311+G(d,p) ^a	–703.71024 1.7	–703.71200 0.6	–703.71301 0.0	–1142.45191 0.0	–1142.45111 0.5	–1142.45044 0.9	–1142.45032 1.0
M06-2X/6-311+G(d,p)	–703.71055 1.7	–703.71234 0.6	–703.71324 0.0	–1142.45206 0.0	–1142.45136 0.4	–1142.45069 0.9	–1142.45051 1.0
M06-2X/6-311+G(d,p)-w ^b	–703.73110 1.5	–703.73318 0.2	–703.73355 0.0	–1142.47543 0.1	–1142.47555 0.0	–1142.47299 1.5	–1142.47415 0.8
							
				–1142.26440 1.3	–1142.26361 1.8		
				–1142.45005 1.2	–1142.44918 1.7		
				–1142.45026 1.1	–1142.44937 1.6		
				–1142.47293 1.6	–1142.47283 1.5		

^a Single-point calculations from M06-2X/6-31G(d)-optimized geometries.

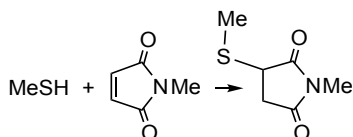
^b Optimized with water as the implicit solvent (CPCM, Spartan'18).

Figure S1. Total energies in au for the low-energy conformers of (*N*-methyl)ethynesulfonamide, $\text{HC}\equiv\text{C}-\text{SO}_2\text{NHMe}$ (upper row), and methyl (*N*-methyl)-phosphonamidate, $\text{HC}\equiv\text{C}-\text{PO}(\text{OMe})\text{NHMe}$ (lower row), and the corresponding adducts with MeSH. Relative energies in bold, in kcal/mol.

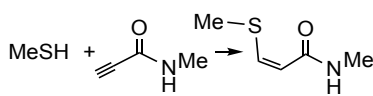
There are no significant differences between the M06-2X/6-311+G(d,p) and M06-2X/6-311+G(d,p)//M06-2X/6-31G(d) energies, as observed in similar substrates and commented above. It is worth noting that, for the adduct of MeSH and methyl (*N*-methyl)ethynephosphonamidate, there are several rotamers very close in energy.

Full Schemes of the main text

Extended Scheme 2. The energy values may be taken as an indirect evaluation of the performance of the different approaches regarding the addition reactions of thiols to activated double and triple bonds. It is observed, as partially commented above or in the main text, that: (1) there is a difference of 15 to 17 kcal/mol in passing from the total energy values to the ΔG° values; (2) M06-2X energies are more negative than CCSD(T)/6-311+G(d,p) energies (ca. -28 kcal/mol for the first reaction and -40.5 kcal/mol for the second reaction, which may be taken as the more reliable values), but the differences are relatively small; (3) at the SCS-MP2/6-311+G(d,p) level the predicted values (-27 and -37 kcal/mol) are less negative than those from the CCSD(T)/6-311+G(d,p) method; (4) when, from the frequency calculations, no corrections are introduced or an approximate scaling factor of 0.95 is included, the ΔH° and ΔG° values undergo changes of only 0.1–0.3 kcal/mol, so that no scaling corrections were considered in the remaining sections of the present work; (5) with different implicit-solvent models, the effect of a very polar solvent such as water was predicted to be insignificant (± 2 kcal/mol) for these reactions, which only involve neutral molecules (however, the SMD method affords ΔE values that are more different from the others); (6) the ω B97X method, with inclusion of dispersion corrections, afforded ΔE values very close to those of CCSD(T)/6-311+G(d,p) for the first reaction and to those of M06-2X for the second reaction; (7) M06-2X/6-311+G(d,p) and M06-2X/6-311+G(d,p)//M06-2X/6-31G(d) give almost the same total energies and reaction energies (differences of 0.0–0.1 kcal/mol); (8) the CCSD(T) total energies arising from B3LYP/6-31G(d) geometries are systematically lower than those arising from M06-2X geometries.



E MP2/6-31G(d) ^a	-437.95246 au	-397.57477 au	-835.57860 au	$\Delta E = -32.3$ kcal/mol
G° MP2/6-31G(d) ^a	-437.93122	-397.51086	-835.47002	$\Delta G^\circ = -17.5$
E MP2/6-311+G(d,p) ^a	-438.03637	-397.78554	-835.87014	$\Delta E = -30.3$
E SCS-MP2/6-31G(d) ^{a,b}	-437.94832	-397.55942	-835.55907	$\Delta E = -32.2$
E SCS-MP2/6-311+G(d,p) ^{a,b}	-438.03963	-397.74771	-835.83035	$\Delta E = -27.0$
E M06-2X ^c	-438.67517	-398.69859	-837.42007	$\Delta E = -29.1$
G° M06-2X (without scaling)	-438.65373	-398.63231	-837.30759	$\Delta G^\circ = -13.5$
H° M06-2X (without scaling)	-438.62421	-398.59428	-837.25805	$\Delta H^\circ = -24.8$
G° M06-2X (scaling factor = 0.95)	-438.65609	-398.63735	-837.31552	$\Delta G^\circ = -13.8$
H° M06-2X (scaling factor = 0.95)	-438.62646	-398.59889	-837.26520	$\Delta H^\circ = -25.0$
E M06-2X-water/CPCM ^d	-438.68057	-398.71191	-837.43674	$\Delta E = -27.8$
E M06-2X-water/SS(V)PE ^d	-438.68049	-398.71175	-837.43369	$\Delta E = -27.7$
E M06-2X-water/CPCM ^e	-438.67898	-398.70844	-837.43197	$\Delta E = -27.0$
E M06-2X-water/SMD ^e	-438.67698	-398.70994	-837.43487	$\Delta E = -30.1$
E ω B97X-D/6-311+G(d,p)	-438.70624	-398.72371	-837.47432	$\Delta E = -27.8$
E M06-2X//M06-2X/6-31G(d)	-438.67516	-398.69850	-837.41982	$\Delta E = -29.0$
E CCSD(T)/6-31G(d)//M06-2X	-437.99318	-397.65317	-835.69325	$\Delta E = -29.4$
E CCSD(T)/6-31+G(d)//B3LYP	-437.99677	-397.68047	-835.72486	$\Delta E = -29.9$
E CCSD(T)/6-31+G(d)//M06-2X	-437.99666	-397.67852	-835.72345	$\Delta E = -30.3$
E CCSD(T)/6-311+G(d,p)//B3LYP	-438.08019	-397.87161	-835.99636	$\Delta E = -28.0$
E CCSD(T)/6-311+G(d,p)//M06-2X	-438.08025	-397.87053	-835.99606	$\Delta E = -28.4$



E MP2/6-31G(d) ^a	-437.95246 au	-284.47065 au	-722.49284 au	$\Delta E = -43.8$ kcal/mol
G° MP2/6-31G(d) ^a	-437.93122	-284.41977	-722.39414	$\Delta G^\circ = -27.0$
E MP2/6-311+G(d,p) ^a	-438.03637	-284.63344	-722.73316	$\Delta E = -39.8$
E SCS-MP2/6-31G(d) ^{a,b}	-437.94832	-284.45971	-722.47787	$\Delta E = -43.8$
E SCS-MP2/6-311+G(d,p) ^{a,b}	-438.03963	-284.61083	-722.70966	$\Delta E = -37.1$
E M06-2X ^c	-438.67517	-285.30679	-724.05057	$\Delta E = -43.1$
G° M06-2X (without scaling)	-438.65373	-285.25194	-723.94828	$\Delta G^\circ = -26.7$
H° M06-2X (without scaling)	-438.62421	-285.21548	-723.90272	$\Delta H^\circ = -39.6$
G° M06-2X (scaling factor = 0.95)	-438.65609	-285.25632	-723.95550	$\Delta G^\circ = -27.0$
H° M06-2X (scaling factor = 0.95)	-438.62646	-285.21950	-723.90928	$\Delta H^\circ = -39.7$
E M06-2X-water/CPCM ^d	-438.68057	-285.32239	-724.07046	$\Delta E = -42.4$
E M06-2X-water/SS(V)PE ^d	-438.68049	-285.32205	-724.06972	$\Delta E = -42.2$
E M06-2X-water/CPCM ^e	-438.67898	-285.31825	-724.06529	$\Delta E = -42.7$
E M06-2X-water/SMD ^e	-438.67698	-285.31981	-724.06843	$\Delta E = -45.0$
E ω B97X-D/6-311+G(d,p)	-438.70624	-285.32683	-724.10154	$\Delta E = -43.0$
E M06-2X//M06-2X/6-31G(d)	-438.67516	-285.30664	-724.05047	$\Delta E = -43.1$
E CCSD(T)/6-31G(d)//B3LYP	-437.99325	-284.53550	-722.59902	$\Delta E = -44.1$
E CCSD(T)/6-31G(d)//M06-2X	-437.99318	-284.53433	-722.59811	$\Delta E = -44.3$
E CCSD(T)/6-311+G(d,p)//B3LYP	-438.08019	-284.70292	-722.84754	$\Delta E = -40.4$
E CCSD(T)/6-311+G(d,p)//M06-2X	-438.08025	-284.70212	-722.84702	$\Delta E = -40.6$

^a Single-point calculations from B3LYP/6-31G(d)-optimized geometries.

^b Calculations with ORCA.

^c M06-2X = M06-2X/6-311+G(d,p), throughout this work.

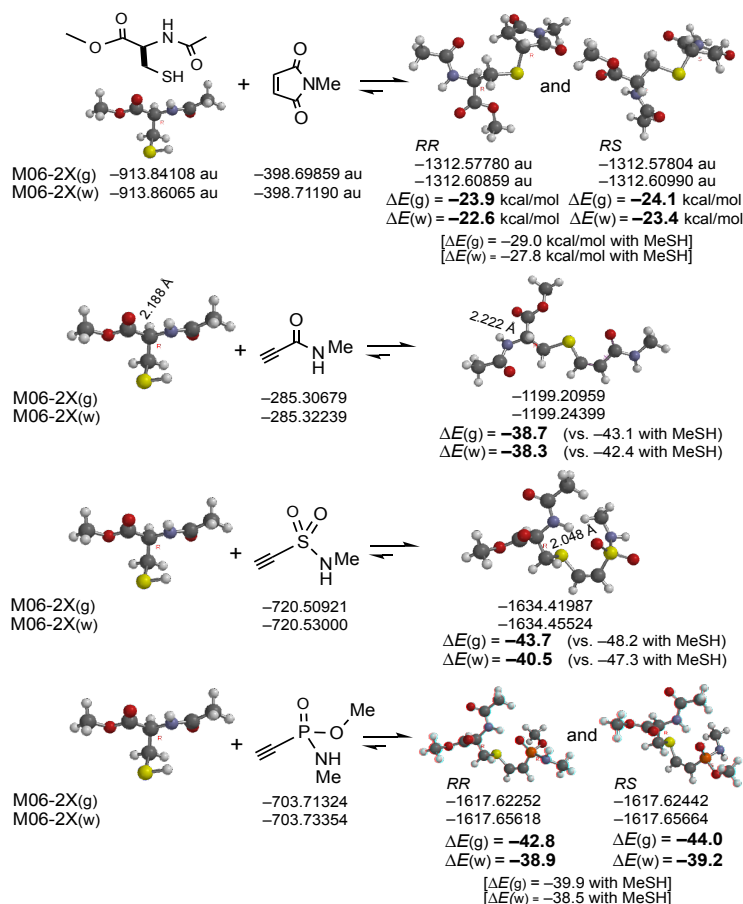
^d Optimization in water with Spartan'18.2. With the SM8 model (with a minimal basis set).

$\Delta E = -31.7$ kcal/mol for the first addition reaction.

^e Optimization in water with Gaussian 16.

Extended Scheme 3. The total energies that appear in the first row are directly obtained by the M06-2X/6-311+G(d,p) method, while those in the second row have been optimized in water as the implicit solvent (CPCM) with the same method. They belong to the lowest-energy conformer of each molecule. This was determined after a standard conformational search by empirical methods, selection of the low energy species from M06-2X/6-31G(d) or MP2/6-31G(d)//B3LYP/6-31(G), and final ordering by means of M06-2X/6-311+G(d,p) or M06-2X/6-311+G(d,p)-w (CPCM), as just mentioned. Not always the lowest-energy conformer of the isolated species (gas phase, in vacuo) was coincident with that obtained in water; such cases are commented in due course.

The reaction energies are given in kcal/mol. All the reactions are exoergic (around -24 kcal/mol for the maleimide, around -40 for the activated triple bonds, in accordance with what was observed for the addition of MeSH). We assume that the corresponding enthalpy energies (Gibbs free energies) would generally be ca. 16 kcal/mol less favorable.

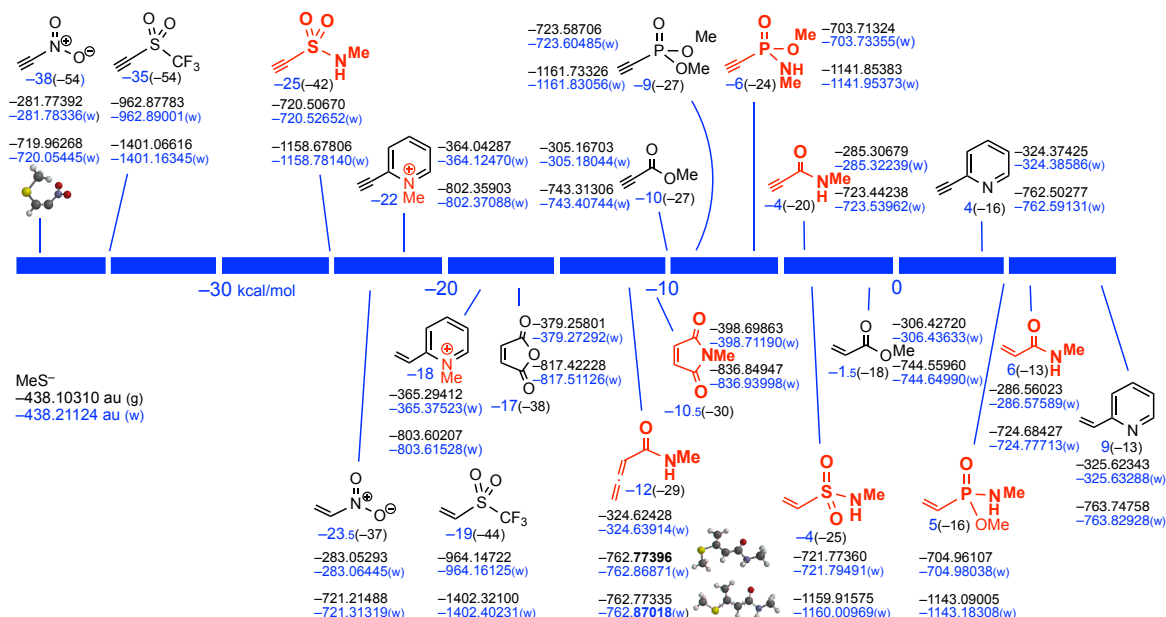


The phosphonamidate case is also included in the expanded Scheme 3. The energy difference between the *RR* and *RS* stereoisomers is predicted to be small, in water. As indicated in Figure S1, there are several conformers very close in energy (a much higher number than in any other case examined by us), due to the tetrahedral arrangement of the substituents bound to the P atom. Another feature is that the energy difference between the adduct of MeSH and that of AcCysOMe was in this case reversed, which we attribute to the network of intramolecular hydrogen bonds (involving the P=O, NHAc, CO groups, NHMe, and OMe groups) that occur in the latter and overstabilize it, especially in the gas phase. Actually, the phosphonamidate case (alkynephosphonamidates, alkenephosphonamidates, allenephosphonamidates...) would require an independent study.

Extended Figure 2. The M06-2X-predicted values for the reaction of addition of MeS⁻ (methanethiolate ion) with optimization in water were collected in Figure 2 of the main text, the details of which are included below. This Figure can be expanded up to 40–50 pairs as we did for the equilibria involving neutral species (Figure 1), but the selection of samples is illustrative of the changes that occur when the anion (MeS⁻) is involved instead of MeSH: the activated double bonds follow a pattern different from that of activated triple bonds. As pointed out in the main text, the energy for the reaction with MeSH is indicative of the thermodynamic stability of the adduct with regard to the retro-Michael reaction (the corresponding E2 mechanism can be favored under basic catalysis and on heating), whereas the energy for the reaction with the anion to give an anionic intermediate is indicative of the kinetics of the process (the lower the energy of such an intermediate, the lower the barrier to reach it).

The total energies in au or Hartrees as directly obtained by M06-2X, that is, by optimization of geometries at the M06-2X/6-311+G(d,p) level, are given in the following extended Figure 2 for each Michael acceptor in the gas phase and optimized in w (CPCM/Spartan'18, in blue), which are the two upper values, and for each adduct, which are the two lower values.

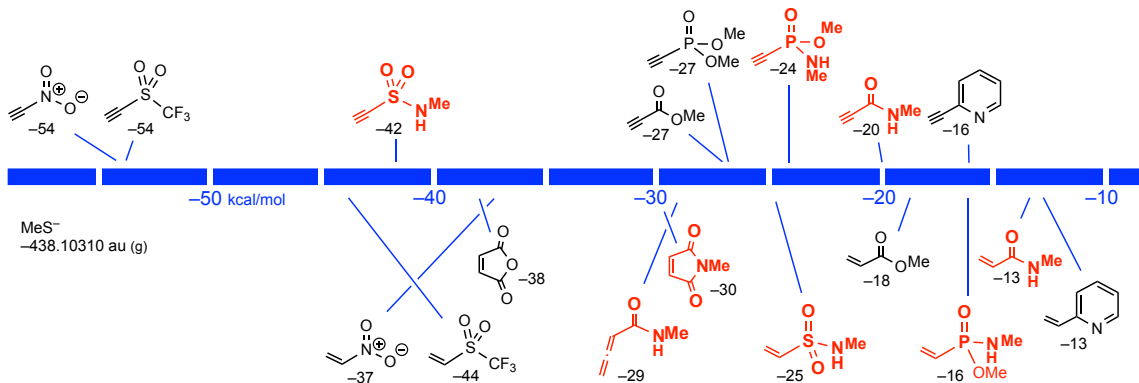
ΔE in kcal/mol, from M06-2X/6-311+G(d,p), in water (in blue) and in the gas phase, for the addition reaction of CH_3S^- to the depicted acceptors



Quite often the lowest-energy anionic adducts adopted a conformation with the MeS folded (due to the electrostatic interaction between the Me group and the partially delocalized negative charge), whereas in water a zigzag conformation (*ap*) of the SMe group turned out often to be that of lowest energy.

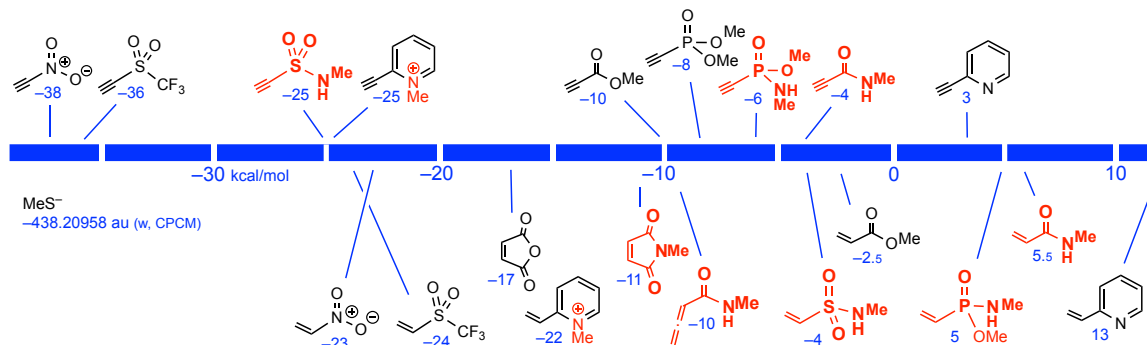
Since, as indicated in the main text, the reliability of some implicit-solvent models is a hot topic under debate, especially when charged molecules are involved, we include below the scale in the gas phase. The relative values are essentially maintained, with a few exchanges of positions (in the next Figure, as shown by the crossing lines, with regard to the preceding Figure, which is Figure 2 of the main text). This may be understood assuming that disparate delocalized anions will not be similarly stabilized by a polar solvent.

ΔE in kcal/mol, from M06-2X/6-311+G(d,p) for the addition reaction of CH_3S^- to the depicted acceptors in the gas phase

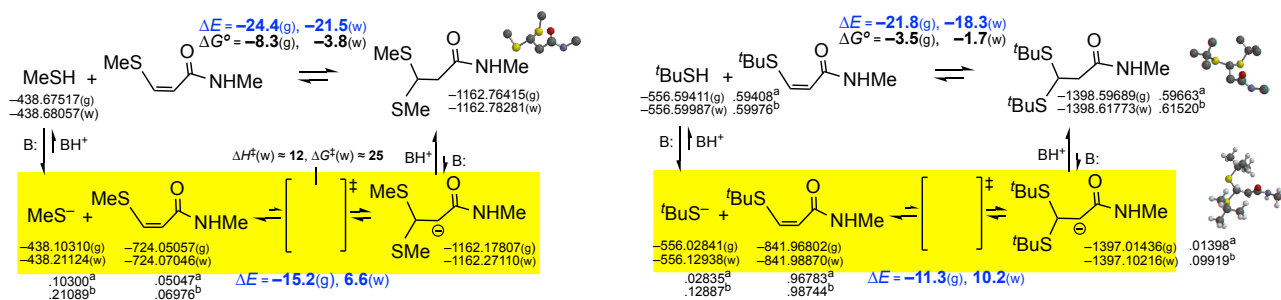


Finally, the following Figure shows the reaction energies in water/CPCM, obtained with Gaussian 16. Despite the fact that the total energies were different, there are almost no changes of position with regard to the first Figure, which indicates that the CPCM parameters implemented in the two packages are qualitatively consistent.

ΔE in kcal/mol, from M06-2X/6-311+G(d,p) in water (CPCM/Gaussian) for the addition reaction of CH_3S^- to the depicted acceptors

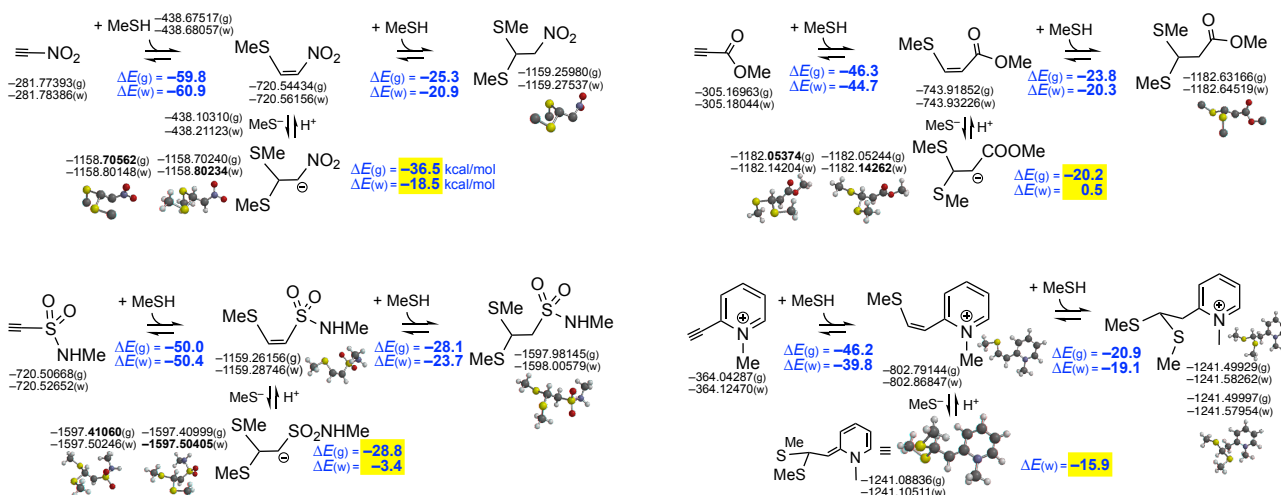


Extended Scheme 9. Kinetically, the second addition of MeS⁻ to *N*-methylpropynamide is unfavorable (see $\Delta E(w) = 6.6$ kcal/mol in Scheme 9, hence $\Delta G^\ddagger(w)$ 22–23 kcal/mol, and see $\Delta G^\ddagger(w) = 25$ kcal/mol; it is even more unfavorable for the case of ^tBuS⁻ (see Scheme 6). Simple steric and electronic effects explain these differences.



M06-2X total energies are in au. Values at the M06-2X/6-311+G(d,p)//M06-2X/6-31G(d) level^a and single-point calculations in water (CPCM, Spartan'18) M06-2X/6-311+G(d,p)-w//M06-2X/6-31G(d)^b are also indicated in several cases, for the sake of comparison: it is observed that the differences are small. Reaction energies are in kcal/mol, as always.

Extended Scheme 10. The M06-2X total energies for the lowest-energy species involved in the first addition of MeSH to representative triple bonds and in the second addition are given in au. The reaction energies obtained from these values are in kcal/mol. In all cases, the second addition, as expected, is predicted to be many kcal/mol less feasible.



AcCysOMe + <i>N</i> -methylpropynamide				AcCysOMe + methyl (<i>N</i> -methyl)ethynephosphonamide, <i>RS</i>				AcCysOMe + methyl (<i>N</i> -methyl)ethynephosphonamide, <i>RR</i>			
1 C C1	0.1524419	-0.8412298	-1.9748661	1 C C1	2.0208634	-0.1252035	-0.5895438	1 C C1	1.8875557	-0.1006031	-0.5112607
2 H H3	-0.6927314	-1.5189001	-1.9043055	2 H H3	2.9669577	-0.5750923	-0.2974426	2 H H3	2.7600198	-0.7169873	-0.3023239
3 S S1	0.4506766	0.1015940	-0.5367788	3 S S1	1.4912078	1.2049537	0.4474435	3 S S1	1.5126459	1.0903661	0.7381695
4 C C6	-0.9798089	-0.5078314	0.4305990	4 C C6	1.6412350	0.3800200	2.0647623	4 C C6	1.5632292	-0.0142350	2.1873886
5 H H2	-1.0300278	-1.5937013	0.3502753	5 H H2	1.8659185	1.1498027	2.8017400	5 H H2	1.8955981	0.5757543	3.0400416
6 H H4	-1.9036560	-0.0620964	0.0555833	6 H H4	2.4578579	-0.3406609	2.0333618	6 H H4	2.2748383	-0.8191139	2.0019209
7 C C7	-0.8419840	-0.1877182	1.9297044	7 C C7	0.3374901	-0.3515643	2.4428194	7 C C7	0.1774950	-0.6259005	2.4672374
8 H H6	0.0813412	-0.6350698	2.3045854	8 H H6	0.5154007	-0.8470596	3.4035896	8 H H6	0.3054746	-1.3453438	3.2844039
9 N N2	-1.9722166	-0.7168303	2.6605288	9 N N2	-0.0724674	-1.3280909	1.4672851	9 N N2	-0.3869356	-1.3029781	1.3279679
10 H H9	-2.6831421	-0.0583886	2.9467363	10 H H9	-0.7861361	-1.0686760	0.7852282	10 H H9	-1.0470947	-0.7899827	0.7422752
11 C C8	-2.0697141	-2.0452118	2.9430781	11 C C8	0.6902636	-2.4339616	1.2614882	11 C C8	0.1888796	-2.4399156	0.8640063
12 O O3	-1.2275943	-2.8419664	2.5754680	12 O O3	1.6841835	-2.6680634	1.9328728	12 O O3	1.1409381	-2.9627472	1.4239957
13 C C9	-3.2789358	-2.4608866	3.7493079	13 C C9	0.2143891	-3.3612582	0.1694090	13 C C9	-0.4388630	-3.0325429	-0.3757737
14 H H12	-2.9322480	-2.8484548	4.7081207	14 H H12	-0.5426136	-2.9002882	-0.4643393	14 H H12	-1.1923209	-2.3772287	-0.8130573
15 H H13	-3.7816178	-3.2731573	3.2246255	15 H H13	-0.1970332	-4.2571007	0.6394274	15 H H13	-0.8904070	-3.9884814	-0.1040164
16 H H14	-3.9818291	-1.6463013	3.9230036	16 H H14	1.0774695	-3.6642183	-0.4238821	16 H H14	0.3547400	-3.2337146	-1.0969763
17 C C10	-0.8140950	1.3130628	2.1598582	17 C C10	-0.7877265	0.6506469	2.6268833	17 C C10	-0.8130757	0.4281441	2.9352864
18 O O4	-1.7811046	1.9627148	2.4631237	18 O O4	-1.8088547	0.6702266	1.9985959	18 O O4	-1.9057543	0.6009976	2.4778242
19 O O5	0.3947906	1.8144617	1.9486293	19 O O5	-0.4804312	1.5422040	3.5780816	19 O O5	-0.3047633	1.1476527	3.9464524
20 C C11	0.4998794	3.2426895	1.9881769	20 C C11	-1.4670861	2.5494382	3.8168140	20 C C11	-1.1669725	2.1642783	4.4643885
21 H H10	0.2345532	3.6090717	2.9795201	21 H H10	-2.4008889	2.0917831	4.1431355	21 H H10	-2.0871510	1.7205231	4.8449367
22 H H17	-0.1655299	3.6828521	1.2459160	22 H H17	-1.6474368	3.1220372	2.9068444	22 H H17	-1.4128007	2.8820600	3.6814672
23 H H18	1.5366722	3.4643079	1.7544207	23 H H18	-1.0567781	3.1849329	4.5966803	23 H H18	-0.6106437	2.6429025	5.2657413
24 C C2	0.8566829	-0.8083322	-3.1139777	24 C C2	1.3789336	-0.5509709	-1.6783179	24 C C2	1.2222150	-0.2387587	-1.6603904
25 H H7	0.5595902	-1.4632074	-3.9258761	25 H H7	1.8189274	-1.3404680	-2.2803430	25 H H7	1.5940207	-0.9441555	-2.3987033
26 C C3	2.0235052	0.0785939	-3.2968569	26 P P1	-0.3230790	-0.1177664	-2.0596481	26 N N1	-0.1493237	2.1637305	-2.0070683
27 O O1	2.4206074	0.8320146	-2.4219096	27 O O1	-1.3380888	-0.7223226	-1.1562729	27 C C5	0.7486816	2.8154552	-2.9552588
28 N N1	2.6409109	-0.0002165	-4.5083852	28 N N3	-0.5223269	-0.6144351	-3.6321984	28 H H1	0.9810354	3.8172890	-2.5967913
29 C C5	3.7839726	0.8411496	-4.8036130	29 H H1	-1.4668632	-0.9167253	-3.8339087	29 H H5	0.3260341	2.8744390	-3.9619822
30 H H1	3.4988834	1.8956984	-4.8302044	30 C C3	0.1680089	0.0681488	-4.7252424	30 H H11	1.6840480	2.2527380	-3.0039686
31 H H5	4.1958010	0.5528035	-5.7698085	31 H H5	1.2141670	0.2173501	-4.4486053	31 H H19	-0.9631203	2.6885014	-1.7151451
32 H H11	4.5462836	0.7162972	-4.0329680	32 H H8	-0.2638139	1.0463851	-4.9535043	32 P P1	-0.3729454	0.5323982	-1.9848285
33 H H19	2.2596435	-0.5978120	-5.2217119	33 H H11	0.1440078	-0.5583267	-5.6166196	33 O O1	-1.4606469	0.0837955	-1.0784008
AcCysOMe + (<i>N</i> -methyl)ethynesulfonamide				34 O O2	-0.3286197	1.4924619	-2.0501762	34 O O2	-0.6276502	0.1373051	-3.5340443
1 C C1	3.0477968	-1.1974218	-0.3820934	35 C C4	-1.3632270	2.2031508	-1.3521999	35 C C3	-1.1067248	-1.1747687	-3.8326471
2 H H3	4.0710319	-0.8406713	-0.4593704	36 H H15	-2.2852307	2.1892090	-1.9360405	36 H H15	-0.3792800	-1.9346446	-3.5302105
3 S S1	2.0367610	-0.4702391	0.8883640	37 H H16	-1.0075604	3.2254779	-1.2436636	37 H H20	-1.2481237	-1.2201347	-4.9100608
4 C C6	1.3951501	0.9629602	-0.0662739	38 H H19	-1.5410192	1.7540239	-0.3745137	38 H H21	-2.0528518	-1.3560936	-3.3205951
5 H H2	1.2407044	0.6378374	-1.0969137								
6 H H4	2.1177417	1.7774129	-0.0315173								
7 C C7	0.0636918	1.4185245	0.5299963								
8 H H6	0.1740384	1.6591611	1.5908325								
9 N N2	-0.9314387	0.3961213	0.3599475								
10 H H9	-0.7755011	-0.3114269	-0.3486830								
11 C C8	-2.1757301	0.5844387	0.8830649								
12 O O3	-2.4302561	1.5361933	1.5960142								
13 C C9	-3.1917709	-0.4803456	0.5412465								
14 H H12	-4.0680148	0.0065989	0.1127241								
15 H H13	-3.5014523	-0.9747832	1.4639095								
16 H H14	-2.8046174	-1.2201778	-0.1604638								
17 C C10	-0.3515223	2.7099970	-0.1818111								
18 O O4	-1.0910960	2.7677753	-1.1208109								
19 O O5	0.2693741	3.7632741	0.3594989								
20 C C11	-0.0444595	5.0273221	-0.2326674								
21 H H10	0.5172237	5.7662844	0.3321741								
22 H H17	-1.1151906	5.2164715	-0.1585252								
23 H H18	0.2502594	5.0360407	-1.2822429								
24 C C2	2.6454639	-2.1547424	-1.2067904								
25 H H7	3.2882585	-2.5981752	-1.9598103								
26 S S2	0.9963850	-2.8435192	-1.2765631								
27 O O1	0.0354611	-1.7565283	-1.3999027								
28 O O2	1.0815384	-3.8728605	-2.2919653								
29 N N1	0.7534317	-3.5780004	0.1872238								
30 H H5	0.8653830	-4.5797243	0.0733811								
31 C C3	-0.3896558	-3.1738163	1.0150106								
32 H H1	-0.2864332	-3.6792285	1.9747304								
33 H H8	-1.3493748	-3.4347556	0.5628400								
34 H H11	-0.3431812	-2.0999972	1.1854464								

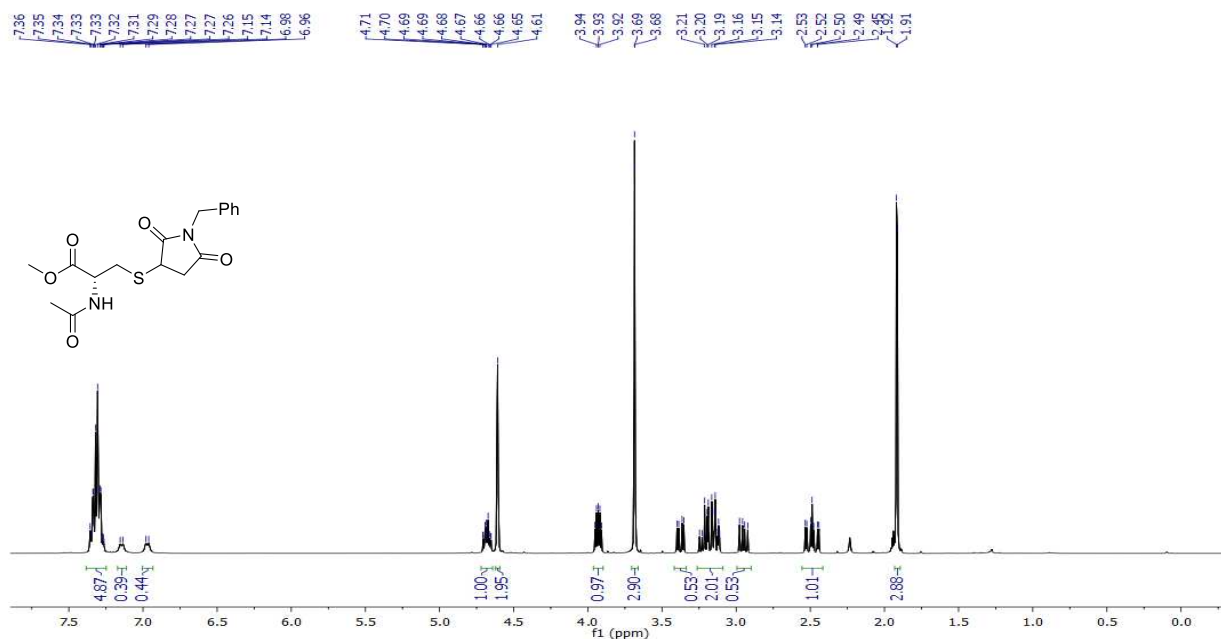
Experimental (for general methods, see Ref S6)

NMR spectra of **1-D**

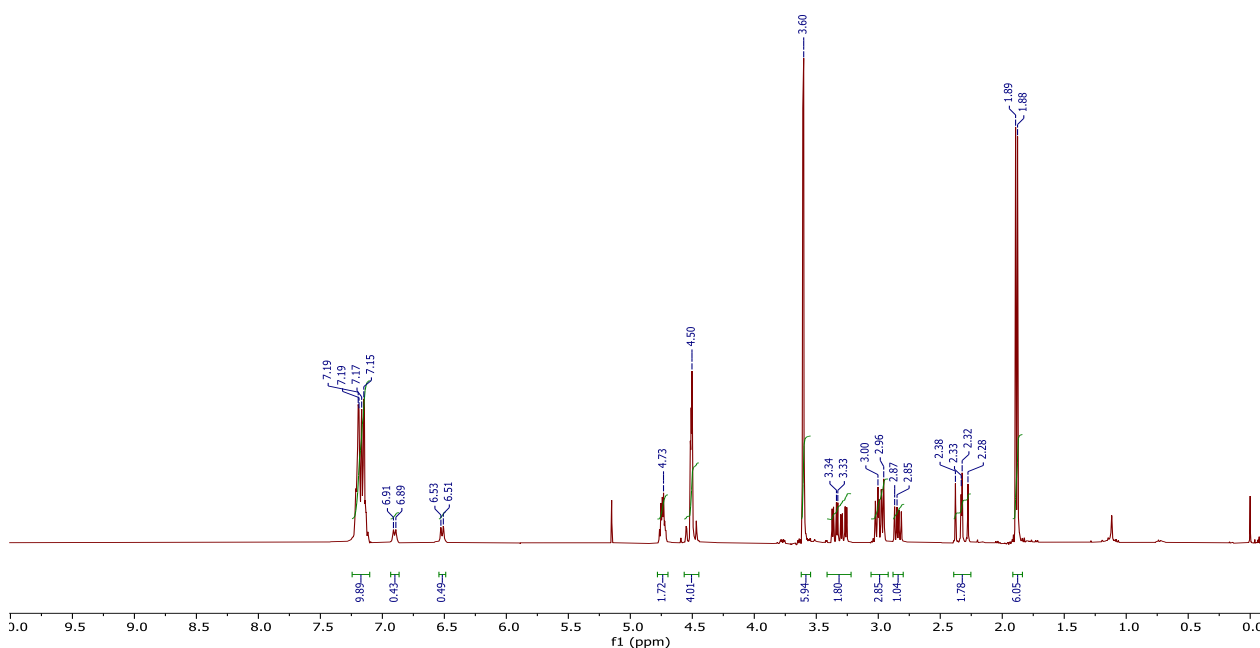
Methyl *N*-acetyl-S-[(3*RS*)-1-phenylmethyl-2,5-dioxopyrrolidin-3-yl]-L-cysteinate, or methyl *N*-acetyl-S-[(3*RS*)-1-benzylmaleimid-4-yl]-L-cysteinate, an almost 1:1 mixture of two diastereomers (**1**), was prepared from commercially available *N*-benzylmaleimide, as reported.^[S5] The addition of a solution of Na₂HPO₄ in D₂O to **1** dissolved in DMSO, quenching with Me₃SiCl/CD₃OD, and partition between water and dichloromethane, gave rise to **1-D**, where the signals of H3', at 3.93 ppm, disappeared and the ¹³C{¹H} signals of C3' at 40.1 and 38.6 ppm changed as expected.

The reaction was also followed by NMR, in DMSO-*d*₆, by addition of a drop of a solution of K₃PO₄ in D₂O (Scheme 5 of the main text); the D/H exchange was quick.

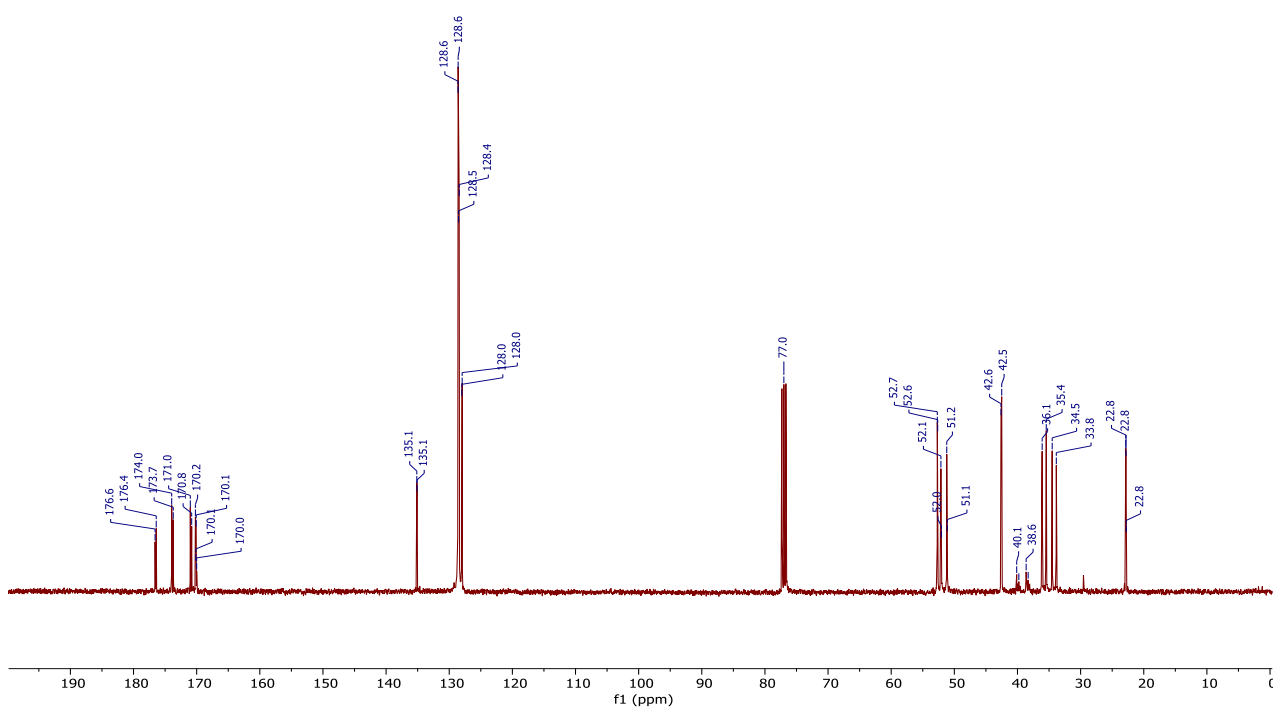
¹H NMR spectrum of **1** (CDCl₃, 400 MHz)



¹H NMR spectrum of **1-D** (CDCl₃, 400 MHz)

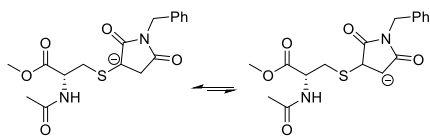
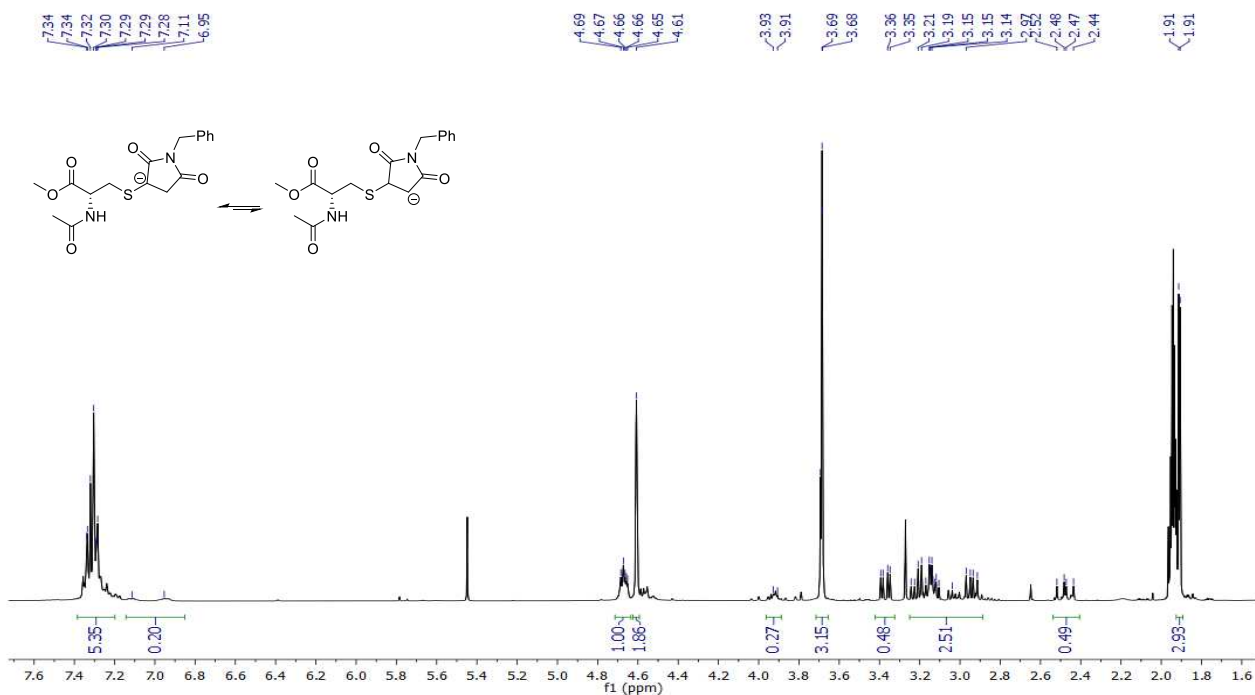


¹³C NMR spectrum of **1**·D (CDCl₃, 100.6 MHz)

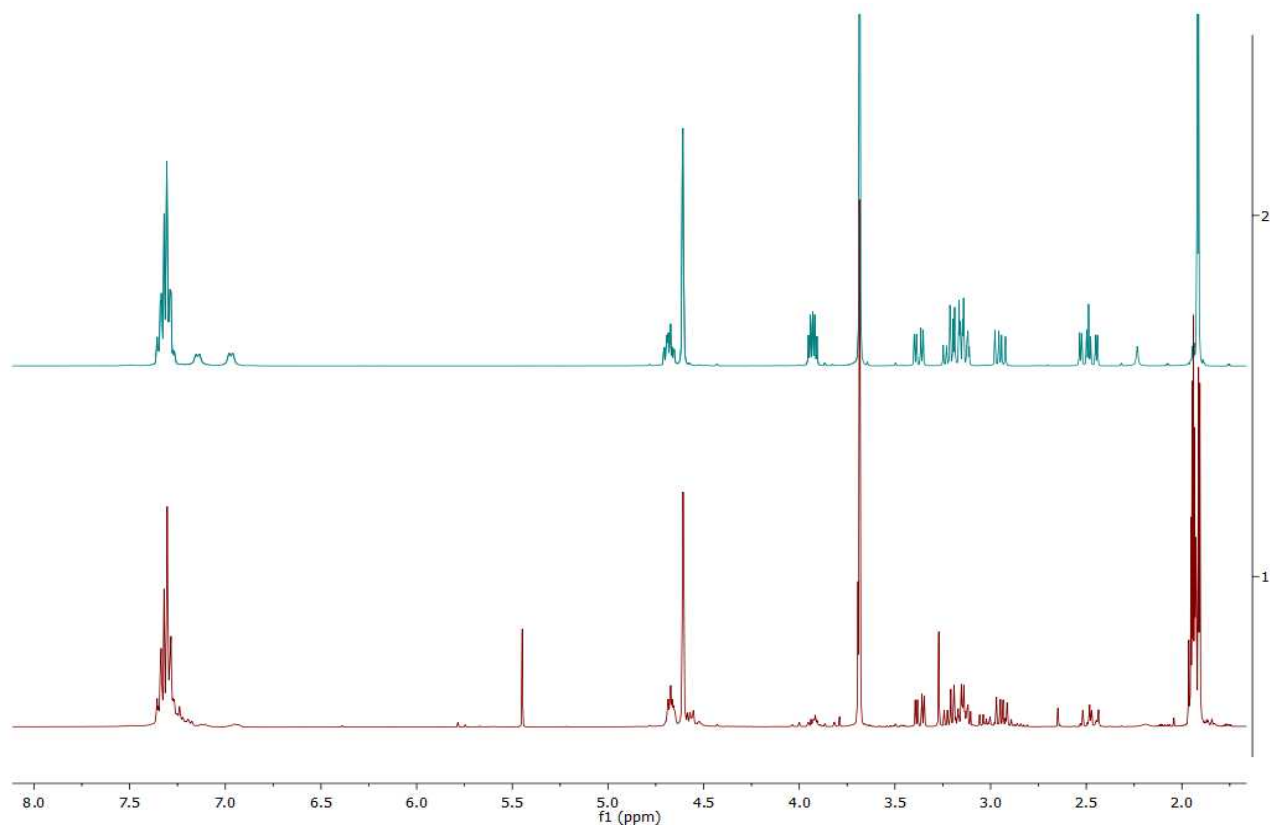


Treatment of **1 with NaH**

Sodium hydride (60% dispersion in mineral oil, ca. 4.00 mg, 0.10 mmol, 0.8 equiv) was added to a solution of **1** (47 mg, 0.13 mmol) in CD₃CN (1.0 mL) (Scheme 5 of the main text). The solution turned dark red. Within 10 min its ¹H NMR spectrum was registered, which was compared with that of the starting material (**1**). The signal at 3.95 ppm (two overlapped dd corresponding to the two diastereomers of **1**) quickly and significantly diminished, but also some percentage of deprotonation of the signals at 2.50 ppm (succinimide methylene) was noted. Although not indicated in the drawings, the NH protons of the acetamido groups of the two diastereomers also disappeared partially.

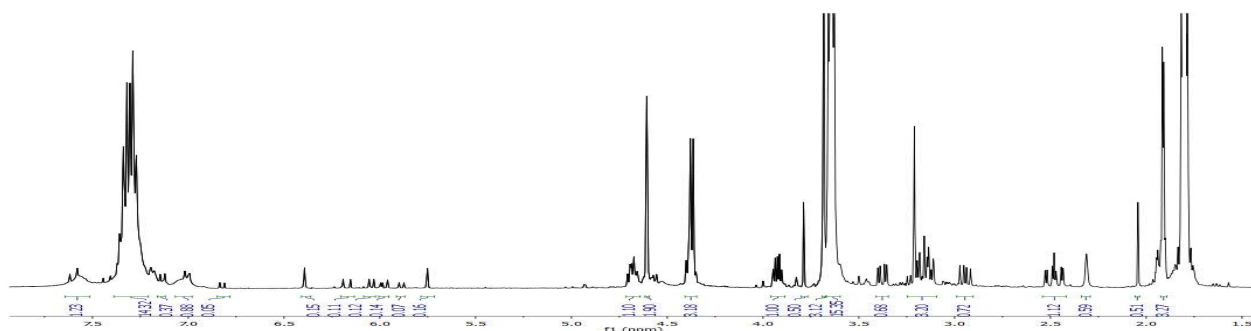


Comparison of the ^1H NMR spectrum of **1** in CD_3CN before and after addition of NaH :



Migration of AcCysOMe from **1** to **2**

tert-Butyllithium (1.7 M in pentane, 16 μL , 27 μmol , 0.1 equiv) was added to a solution of **1** (98 mg, 0.27 mmol) and *N*-benzylpropynamide (**2**, 43 mg, 0.27 mmol) in anhydrous THF (3.0 mL) under N_2 atmosphere, at -78°C . The reaction was then stirred at room temperature for 2 h. After neutralization with aqueous phosphate buffer, extraction with dichloromethane (x 3), and drying of the combined organic layers, the organic solvents were removed under reduced pressure (rotary evaporator). The ^1H NMR spectrum of the crude mixture was registered in CDCl_3 .



Double bonds (of known^[55] AcCysOMe(S)-CH=CH-CONHBn, **Z-3** + **E-3**, around 10%) are observed. Also the signal of the double bond of *N*-benzylmaleimide (at 6.45 ppm) appeared, in 5–10%. The formation of these compounds was confirmed by TLC and MS.

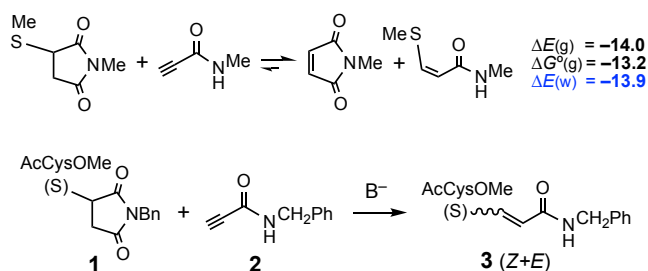
tert-Butyllithium (1.7 M, 165 μL , 280 μmol , 0.85 equiv) was added to a solution of **1** (120 mg, ca. 0.33 mmol) and **2** (52 mg, 0.33 mmol) in anhydrous THF (3.5 mL) under N_2 atmosphere, at -78°C . The solution, which immediately turned dark red, was stirred for 2 h at room temperature. After neutralization, extraction with CH_2Cl_2 , and drying of the combined organic solutions, the solvent was removed under reduced pressure. The residue was chromatographically compared with pure samples of the expected products and was analyzed by ^1H NMR spectroscopy to contain **Z-3** + **E-3** (ca. 70%) and polymeric material rather than *N*-benzylmaleimide.

Exchange of thiolates in the maleimide adducts (mechanisms)

Formally, an exchange of MeSH between the methylsulfanylsuccinimide shown in Scheme S1 and any propynamide is feasible. The hypothetical equilibrium must be shifted very far to the right; it will suffice to find a suitable catalyst and/or to reach the appropriate temperature.

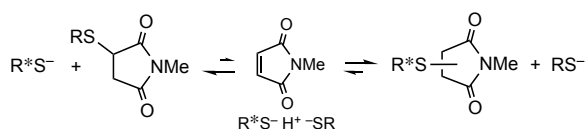
In vitro, when succinimide **1** and *N*-benzylpropynamide (**2**) were mixed in CH₃CN at rt plus a catalytic amount of Na⁺DMSO⁻ or in THF at -78 °C plus ^tBuLi (either in catalytic or substoichiometric amounts), the formation of **3** (*Z/E* mixture) was rapidly and clearly observed by TLC and NMR. The exchange takes place, in agreement with the predictions, but in the absence of a source of protons it cannot be avoided that the generated allenolate-type ion, during the workup, gives rise to the *Z/E* mixture instead of the *Z* isomer. The coproduct from the exchange, *N*-benzylmaleimide, could not be isolated as it undergoes a rapid polymerization (formation of a dark red polymer) in non-aqueous basic media.⁵⁷

Scheme S1. Plausible exchange reaction on the basis of M06-2X calculations. ΔE and ΔG° values in kcal/mol, in bold. Reaction of **1** and **2** in the presence of strong bases



If the elimination of RS⁻ (E1cB, from the minor succinimide anion with the negative charge at C4, see Scheme 4) or of RSH (E2, from the neutral adduct, under basic catalysis) occurs, the generated species, RS⁻, will immediately react with the ynamide. In aqueous solutions, this reversal or retro-Michael reactions is assumed for the exchange of thiols in Cys-maleimide-containing ADCs. As shown in Scheme S2, there is a series of equilibrium reactions with very small barriers (as predicted in Scheme 4).

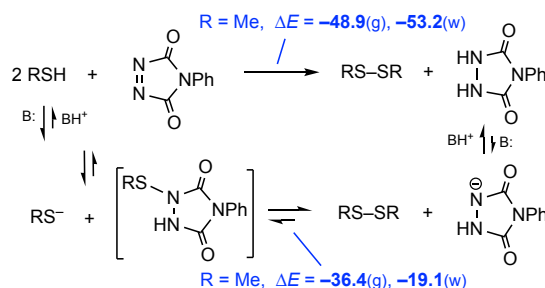
Scheme S2. Exchange reactions via elimination–addition steps



Other reactions of alkylsulfanyl derivatives are possible. When the acceptors are strong, as in the case of 4-phenyl-1,2,4-triazoline-3,5-dione (PTAD), and the new bond (S–N) is weaker than a standard S–C bond, it is known that a second unity of thiol or thiolate causes the formation of dialkyl disulfide,⁵⁸ as shown in Scheme 12.

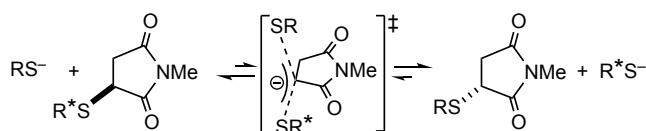
We have calculated the energies of these species for the case of the methanethiolate ion (MeS⁻). The overall reaction is highly exothermic (Scheme S3), as are all the individual steps. In contrast, for the parallel reaction of MeS⁻ with the adduct from *N*-methylmaleimide, the reaction cannot work: the value of $\Delta E(g)$ was 3.7 kcal/mol and that of $\Delta E(w)$ 18.7 kcal/mol (both positive).

Scheme S3. Known reaction of dimerization of thiols, mediated by very strong acceptors, which probably pass through the Michael adduct, followed by the formation of the S–S bond. Values of ΔE in kcal/mol



Another possibility is that a S_N2 mechanism is involved, such as the identity reaction⁵⁹ depicted in Scheme S4, where the substitution would be relatively favored as it occurs at position α to a carbonyl group. We investigated the TS for such a simple S_N2 reaction (Scheme S4, with R = R* = Me). With M06-2X, in the gas phase, the energy of the located TS was around 3 kcal/mol above the sum of the energies of the individual components (quite a low barrier), whereas in water it was 26 kcal/mol above them (quite a high barrier). The nature of the TS, which is much less polar than MeS⁻, explains this large effect of the solvent polarity. With larger thiolate ions the effect of water is expected to be less significant.

Scheme S4. Alternative mechanism (a standard S_N2) for the exchange of thiols



Attempted experiments to gain more insight into the exchange mechanisms in vitro, with partially deuterated adducts and lithium 1-dodecanethiolate, were not conclusive. The known tendency of succinimide intermediates to undergo ring opening in basic aqueous media and of maleimides to undergo anionic polymerization in non-protic media were prevalent.

References

- (S1) Gaussian 16, Revision C.01, <https://gaussian.com>. Frisch, M. J.; Trucks, G. W.; Schlegel, H. B.; Scuseria, G. E.; Robb, M. A.; Cheeseman, J. R.; Scalmani, G.; Barone, V.; Petersson, G. A.; Nakatsuji, H.; Li, X.; Caricato, M.; Marenich, A. V.; Bloino, J.; Janesko, B. G.; Gomperts, R.; Mennucci, B.; Hratchian, H. P.; Ortiz, J. V.; Izmaylov, A. F.; Sonnenberg, J. L.; Williams-Young, D.; Ding, F.; Lipparini, F.; Egidi, F.; Goings, J.; Peng, B.; Petrone, A.; Henderson, T.; Ranasinghe, D.; Zakrzewski, V. G.; Gao, J.; Rega, N.; Zheng, G.; Liang, W.; Hada, M.; Ehara, M.; Toyota, K.; Fukuda, R.; Hasegawa, J.; Ishida, M.; Nakajima, T.; Honda, Y.; Kitao, O.; Nakai, H.; Vreven, T.; Throssell, K.; Montgomery, J. A., Jr.; Peralta, J. E.; Ogliaro, F.; Bearpark, M. J.; Heyd, J. J.; Brothers, E. N.; Kudin, K. N.; Staroverov, V. N.; Keith, T. A.; Kobayashi, R.; Normand, J.; Raghavachari, K.; Rendell, A. P.; Burant, J. C.; Iyengar, S. S.; Tomasi, J.; Cossi, M.; Millam, J. M.; Klene, M.; Adamo, C.; Cammi, R.; Ochterski, J. W.; Martin, R. L.; Morokuma, K.; Farkas, O.; Foresman, J. B.; Fox, D. J. Gaussian, Inc., Wallingford CT, 2016.
- (S2) (a) Spartan'18.2, <https://www.wavefun.com>. Deppmeier, B.; Driessen, A.; Hehre, T.; Hehre, W.; Klunzinger, P.; Ohlinger, S.; Schnitker, J. Wavefunction, Inc., 18401 Von Karman Avenue, Irvine, CA 92612. (b) ORCA 4.2.1, <https://orcaforum.kofo.mpg.de/app.php/portal>. Neese, F.; Wennmohs, F.; Becker, U.; Riplinger, C. The ORCA Quantum Chemistry Program Package. *J. Chem. Phys.* **2020**, *152*, 224108-1–224108-18.
- (S3) (a) Zhao, Y.; Truhlar, D. G. *Theor. Chem. Acc.* **2008**, *120*, 215–241. (b) Zhao, Y.; Truhlar, D. G. *Acc. Chem. Res.* **2008**, *41*, 157–167.
- (S4) (a) Castro-Alvarez, A.; Carneros, H.; Sánchez, D.; Vilarrasa, J. *J. Org. Chem.* **2015**, *80*, 11977–11985. (b) Castro-Alvarez, A.; Carneros, H.; Calafat, J.; Costa, A. M.; Marco, C.; Vilarrasa, J. *ACS Omega* **2019**, *4*, 18167–18194.
- (S5) <https://cccbdb.nist.gov/vibscalejust.asp>
- (S6) Petit, E.; Bosch, L.; Costa, A. M.; Vilarrasa, J. *J. Org. Chem.* **2019**, *84*, 11170–11176.
- (S7) (a) Oishi, T.; Onimura, K.; Isobe, Y.; Yanagihara, H.; Tsutsumi, H. *J. Polym. Sci. Part A: Polym. C* **2000**, *38*, 310–320 (and references therein). For very recent reviews, see: (b) Oz, Y.; Sanyal, A. *Chem. Rec.* **2018**, *18*, 570–586. (c) Dolci, E.; Froidevaux, V.; Joly-Duhamel, C.; Auvergne, R.; Boutevin, B.; Caillol, S. *Polym. Rev.* **2016**, *56*, 512–556.
- (S8) The reaction works with DEAD and related azo derivatives conjugated with EWGs, including PTAD: (a) Harasawa, S.; Yoshida, K.; Kojima, C.; Araki, L.; Kurihara, T. *Tetrahedron* **2004**, *60*, 11911–11922. (b) Christoforou, A.; Nicolaou, G.; Elemes, Y. *Tetrahedron Lett.* **2006**, *47*, 9211–9213. (c) Morais, G. B.; Falconer, R. A. *Tetrahedron Lett.* **2007**, *48*, 7637–7641. For reviews of the formation of RSSR', see: (d) Mandal, B.; Basu, B. *RSC Adv.* **2014**, *4*, 13854–13881. (e) Wang, M.; Jiang, X. *Top. Curr. Chem.* **2018**, *376*, 1–40. For the addition of MeSH to dimethyl azodicarboxylate, our M06-2X calculations predict $\Delta E(g) = -34.5$ kcal/mol and $\Delta E(w) = -38$ kcal/mol; for that of MeS⁻, $\Delta E(g) = -41$ kcal/mol and $\Delta E(w) = -30$ kcal/mol; these last values are lower than those of PTAD (Scheme S3).
- (S9) (a) Gonzales, J. M.; Allen, W. D.; Schaefer III, H. F. *J. Phys. Chem. A* **2005**, *109*, 10613–10628. (b) Hoz, S.; Basch, H.; Wolk, J. L.; Hoz, T.; Rozental, E. *J. Am. Chem. Soc.* **1999**, *121*, 7724–7725. (c) Shaik, S. S. *J. Am. Chem. Soc.* **1984**, *106*, 1227–1232.